

## Core-electron spectroscopy of adsorbate ions: Iodine on Ag(111)

G. K. Wertheim, S. B. DiCenzo, and D. N. E. Buchanan

*Bell Laboratories, Murray Hill, New Jersey 07974*

(Received 9 November 1981)

Submonolayer coverages of iodine deposited on clean Ag(111) have been studied by x-ray photoelectron spectroscopy. The adsorbate core-electron binding energy is found to be 0.1-eV smaller at saturation than in the dilute limit, indicating that the iodine carries only a small negative charge. The low-energy electron diffraction evidence for clustering of the adatoms into the  $\sqrt{3} \times \sqrt{3}$  structure at coverages considerably less than  $\frac{1}{3}$  monolayer is confirmed by the observation, at those coverages, of a constant  $I4d$  binding energy. The excitation of silver surface plasmons by the core ionization of the adsorbate has also been observed.

## I. INTRODUCTION

Core-electron spectroscopy of ions adsorbed on clean surfaces probes both the initial chemical state of the adsorbate and the dynamic response of the substrate to the creation of a core hole. Both aspects are of fundamental interest. We have recently shown that the charge state of the adsorbate ion can be obtained from the coverage dependence of the adsorbate core-electron binding energy.<sup>1</sup> The final state aspects have received detailed theoretical attention in recent years.<sup>2-4</sup>

The system I on Ag(111) was chosen for a study of these phenomena because it has been well characterized by low-energy electron diffraction (LEED)<sup>5</sup> and surface EXAFS.<sup>6</sup> The structure of the saturated adsorbate layer, the adsorption site, and the bond length are known. Since the last is close to the sum of the covalent radii, the charge of the adsorbate ion should be small.

## II. EXPERIMENTAL

The substrate used in these experiments was an ordered epitaxial layer of silver grown on mica. A  $1.0 \times 1.2$ -cm<sup>2</sup> specimen was introduced into a sample preparation chamber attached to a HP 5950A spectrometer, and cleaned by argon ion sputtering and annealing. According to the LEED pattern the resulting surfaces were well ordered (111) planes. XPS scans showed that they were free of oxygen contamination, but generally had some detectable residual carbon. The iodine overlayer was established by admitting iodine into the preparation chamber through a leak valve to a pressure of  $10^{-6}$  Pa, while the LEED pattern was being observed. XPS data were taken at various stages of surface preparations: (1) prior to the deposition of iodine, (2) after exposure to iodine but before significant changes could be observed in the LEED pattern, and (3) with well-

defined  $\sqrt{3} \times \sqrt{3}R$  30° pattern corresponding, at saturation, to a  $\frac{1}{3}$  monolayer coverage. Prolonged exposure beyond that required to produce the  $\frac{1}{3}$  coverage leads to the occurrence of inequivalent I in the adsorbed layer, judging by the broadening of the iodine XPS lines. Such surfaces will not be considered here.

Since XPS is inherently a surface sensitive technique, the detection of fractional monolayers of adsorbate presents little difficulty. The photoelectron spectra of the  $I3d$  and  $Ag3p_{1/2}$  core electrons of a sample which gave a good  $\sqrt{3} \times \sqrt{3}$  LEED pattern are shown in the top of Fig. 1. The spectrum of a clean Ag surface is shown below. The iodine coverage can be estimated from the areas of the photoemission lines, provided the escape depth and photoelectric cross sections are known. The areas under the  $I3d$  and  $Ag3p_{1/2}$  parts of the spectrum are in a ratio  $A$  of 1.33. The corresponding cross section ratio  $R_\sigma$  according to the tabulations of Scofield,<sup>7</sup> is 8.35. The escape depth  $\lambda$  for electrons with circa 900 eV kinetic energy in silver<sup>8</sup> is 7 Å. The coverage  $\Theta$  is then given by  $A \lambda \cos(\phi) / d_{111} R_\sigma$ , where  $d_{111}$  is the 2.354 Å spacing of the Ag (111) planes, and  $\phi$  is the angle between the normal to the sample surface and the direction to the entrance slit of the electron spectrometer (52° in the HP spectrometer). Finally, the attenuation of the signals by the overlayer must be taken into account. A 15% correction is determined from the observed attenuation of the  $Ag3p$  signal in the spectrum of Fig. 1, yielding an estimated coverage of 0.25 monolayer.

An alternative calibration is obtained by using the LEED pattern to confirm that the adsorbate has the  $\sqrt{3} \times \sqrt{3}$  structure, and the XPS intensity and line shape to indicate that the coverage has reached but not exceeded the saturation value. The strength of the  $I3d$  signal obtained in that case is taken as representative of  $\frac{1}{3}$  coverage. The fractional intensity obtained for other exposures then provides a direct

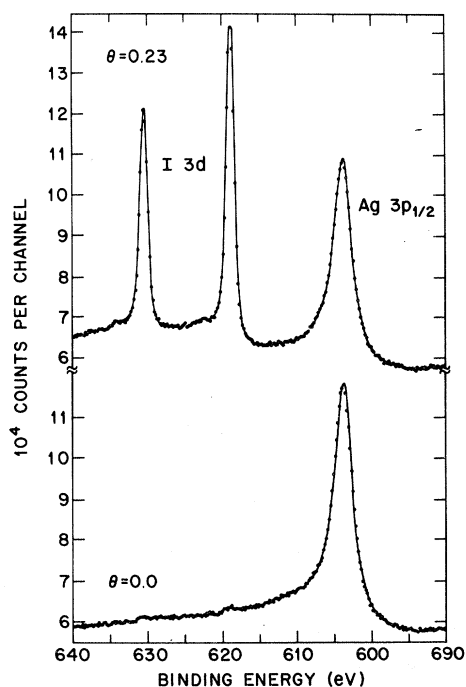


FIG. 1. X-ray photoemission spectra of clean silver and silver with 0.23 monolayers of iodine, in the  $I\ 3d$  and  $Ag\ 3p_{1/2}$  region.

measure of coverage. This method suffers from the weakness that it is not known how close to saturation the coverage is at the observed maximum in XPS intensity. This calibration gave a coverage of 0.23 for the surface shown in Fig. 1, somewhat smaller than the estimate obtained by the first method, but in satisfactory agreement considering the inherent uncertainties. In the subsequent discussion we will use coverages determined by the second method because they do not depend on the escape depth in the substrate, a quantity which is not known with great confidence.

The binding energies reported in this paper were all referenced to the Fermi energy of the substrate. This energy was initially determined from the valence band spectrum of each surface studied. It provides a reference level which is independent of changes in the work functions of the sample and spectrometer. It also removes any changes in energy scale due to slow instrumental drift or differences in the heights of the various samples, the latter sensitivity arising in the HP spectrometer from the use of dispersion compensation. The Fermi energy was determined by fitting a theoretical Fermi cutoff shape to valence band data. It is worth noting here that the valence band spectra were not significantly modified by the adsorption of iodine. Neither the shape of the  $4d$  band, nor its position relative to the Fermi energy changed

measurably with coverage, indicating that the  $4d$  states are not affected by the iodine. This is not surprising since most of the intensity in the valence band spectrum reflects properties of silver atoms in the bulk, and these are certainly not affected by the adsorbate. The only change which could be detected at higher coverages was the appearance of a weak contribution from the iodine  $5p$  states, beginning about 2 eV below the Fermi energy.

### III. DATA ANALYSIS

The binding energy of the  $Ag\ 3d_{5/2}$  line was obtained by fitting a Doniach-Sunjić<sup>9</sup> line to the data and expressing the binding energy relative to the Fermi level. The average value resulting from these measurements is 368.21 eV, with an 0.015-eV rms deviation, see Fig. 2(a). This provides a measure of the instrumental stability and the reliability of the individual least-squares determinations. It also indicates that the binding energy of the first atomic layer of silver, which provides circa 15% of the signal, is not changed by more than 0.1 eV.

The lifetime width of the  $Ag\ 3d$  line was found to be 0.3 eV full width at half maximum (FWHM) in agreement with an earlier work<sup>10</sup> which gave 0.28 eV. The width of the  $Ag\ 3d$  line did not change measurably with iodine coverage, giving confirmation that the core-electron binding energy of the first atomic layer is not significantly changed by the adsorbate. The singularity index is not determined with high accuracy in these experiments because of some uncer-

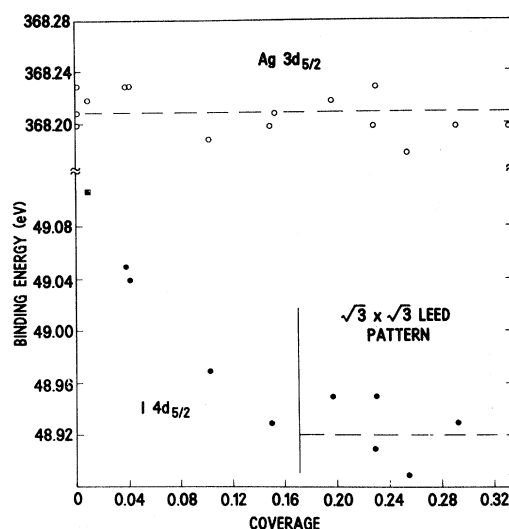


FIG. 2. Binding energies of  $Ag\ 3d_{5/2}$  and  $I\ 4d_{5/2}$  on  $Ag(111)$  as a function of coverage. The data are referenced to the experimentally determined Fermi level.

tainty in the asymmetry of the instrumental resolution function. A value somewhat larger than the 0.06 which is believed to be reliable<sup>11,12</sup> was typically obtained, but the difference is not considered significant.

The Ag 3*d* spectra clearly exhibit the plasmon satellite, which has been previously identified as the 3.78-eV surface plasmon.<sup>13</sup> The surface plasmon energy was found to decrease slightly with iodine coverage. In Fig. 3 we show, on a logarithmic scale, the Ag 3*d* spectra of the two samples whose I 3*d* spectra are shown in Fig. 1. The decrease of the plasmon energy with coverage is made more evident by superimposing the plasmon region of the clean sample on that of the one with adsorbate as a dashed line. Such coverage dependent shifts of surface plasmon energies are well known. A discussion in terms of free-electron plasmon theory is inappropriate because the silver plasmons have significant interband character.

The silver surface plasmon can also be seen directly on the adsorbate I 3*d* lines, Fig. 4. The plasmon energy is in good agreement with that found for the Ag 3*d* line for the same exposure. The surface plasmon is less evident on the I 4*d* lines because the 4*d*<sub>3/2</sub> line falls between the 4*d*<sub>5/2</sub> line and its plasmon, as seen in Fig. 5.

The I 3*d* lines, which exhibit the surface plasmon most clearly, are not well suited for more detailed studies because their lifetime width is relatively large. For further analysis, the I 4*d* doublet at 50 eV is preferable even though its photoelectric cross section<sup>7</sup> is smaller by a factor of 8. The smaller lifetime width compensates in part for the smaller cross section by increasing the peak height.

Although the I 4*d* doublet lies well below the Ag 4*p* lines at 60 eV, the Lorentzian tail of the Ag line is

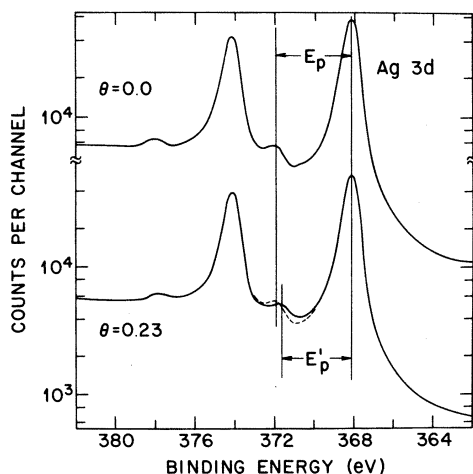


FIG. 3. Ag 3*d* spectra of clean and iodine covered silver, showing the change in the surface plasmon energy.

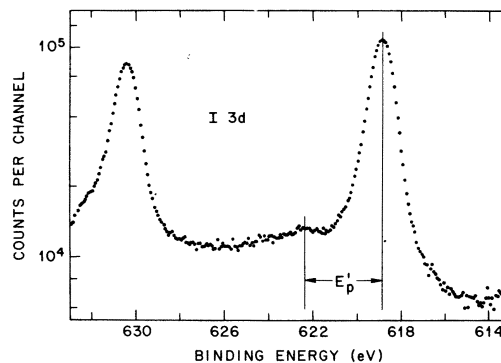


FIG. 4. I 3*d* spectrum of Ag(111) covered with 0.23 monolayers of iodine. The Ag surface plasmon is indicated.

not negligible in the I 4*d* region. In order to carry out a least-squares analysis of the I line, the silver background must be included in the model function which is fitted to the data. Rather than resort to a mathematical representation of this background, we have used an actual background spectrum of the same binding energy interval, measured with a freshly cleaned sample and smoothed to remove the residual statistical fluctuations. The resulting background was used with an adjustable weight factor in the model function which was fitted to the data. This

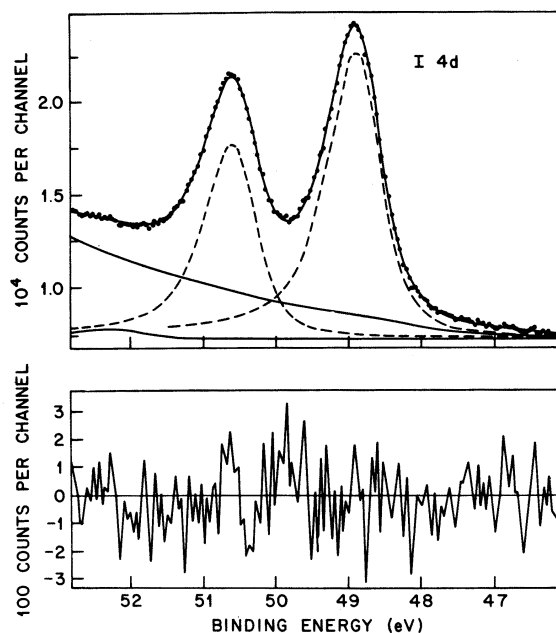


FIG. 5. Least-squares analysis of the I 4*d* lines of a Ag(111) surface with 0.23 monolayers of adsorbed iodine (see text for details).

is more reliable than subtracting the Ag background spectrum and then fitting the data, both because the I signal is small compared to the background, and because the strength of the Ag background, which depends on the attenuation by the overlayer, is not known *a priori*. The 4*d* lines were represented by the Doniach-Sunjic equation<sup>9</sup> which contains the power-law character of the surface screening response as given in various theoretical treatments.<sup>2-4</sup> The useful range of the model was extended by including the 3.78-eV surface plasmon<sup>14,15</sup> energy loss in the model function as a separate line with independent parameters. This is called for by earlier work, both theoretical<sup>2-4</sup> and experimental.<sup>16-18</sup>

An example of a fit obtained with this model is shown in Fig. 5, which also displays the four components of the curve through the data points. The residuals are shown below the main figure. The fit determines ten parameters. Five describe the I4*d*<sub>5/2</sub> component in terms of its position, amplitude, lifetime width, singularity index, and phonon width. Two define the I4*d*<sub>3/2</sub> component in terms of its shift and amplitude relative to the  $\frac{5}{2}$  component; thus, it is assumed to have the same shape as the  $\frac{5}{2}$  component. Two define the amplitude and width of the surface plasmon satellites, whose excitation energy ranges from 3.78 eV for a clean Ag surface to 3.6 eV for  $\frac{1}{3}$  coverage. One defines the amplitude of the Ag background spectrum, obtained as described above. The essential numerical results are given in Table I. It is worth noting that the residuals show only random statistical fluctuations and no structure related to the data themselves, as is essential if one is to have any confidence in the parameters determined by such a fit. This also confirms that the model function provides an adequate representation of the data, i.e., that the Doniach-Sunjic function adequately represents the screening response of the substrate. Finally, it should be noted that the position of the  $\frac{5}{2}$  component is clearly not sensitive to the details of the model, since the background is relatively flat and the plasmon contribution negligible in its vicinity. This is important for the discussion below, which will consider the origin of small changes in the binding energy of this line.

The binding energies of I4*d*<sub>5/2</sub> for all the surfaces which were examined are shown as a function of coverage in Fig. 2(b). Comparison with the data for Ag 3*d* above shows a significant correlation in the fluctuations from the average line, indicating that the largest uncertainty in the binding energies arises from the determination of the Fermi energy. This source of error can be circumvented by using the Ag 3*d* line as the reference level, and placing the Fermi level 368.21 eV below its energy. The I4*d* binding energies are replotted with this reference in Fig. 6.

In further discussion we will ignore the point at

TABLE I. Parameters derived from least-squares analysis of Ag 3*d* and I4*d* lines.

	Ag 3 <i>d</i>	I4 <i>d</i>
$E_B^a$	368.21 ± 0.02	48.92 ± 0.03
SO splitting <sup>b</sup>	6.01 ± 0.01	1.71 ± 0.02
ratio	0.67	0.69
$\Gamma_{nat}^c$	0.27 ± 0.10 eV	0.35 ± 0.15 eV
$\alpha^d$	[0.06]	0.045 ± 0.015

<sup>a</sup>Binding energy of *d*<sub>5/2</sub> line relative to  $E_F$ , in electron volts.

<sup>b</sup>Spin-orbit splitting in electron volts.

<sup>c</sup>Lifetime width, as FWHM, in electron volts.

<sup>d</sup>Singularity index. The value for Ag 3*d* is from Ref. 11 and 12.

lowest coverage, which was obtained from iodine which remained after an attempt at cleaning the sample. The remaining data distinctly show the binding energy decreasing with coverage up to  $\Theta = 0.2$ , and then remaining constant. The region of constant binding energy coincides with the region in which the  $\sqrt{3} \times \sqrt{3}$  LEED pattern was observed. These two observations strongly suggest that in this region most of the adsorbate atoms are in islands or clusters of the  $\sqrt{3} \times \sqrt{3}$  structure. The energy shift between the most dilute coverage and this ordered coverage is only 0.11 eV; however, this shift is much greater than the typical experimental uncertainty of 0.02 eV. Since the observed shift is much smaller than the experimental line width (see Fig. 5), the measured binding energy may represent an average for isolated iodine atoms and those in clusters, especially at the lower coverages.

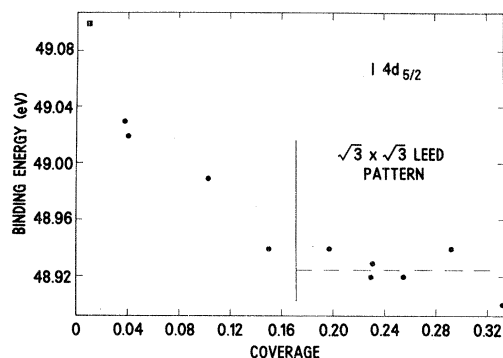


FIG. 6. Binding energy of I4*d*<sub>5/2</sub> on Ag(111), referenced to  $E_F$  defined to lie 368.21 eV below the Ag 3*d*<sub>5/2</sub> line.

#### IV. DISCUSSION

In many ways the most interesting result is the coverage dependence of the  $I4d$  core-electron binding energy, which reflects interactions between adsorbate ions in both the initial and the final state. The final state contributes through the relaxation of the atom itself and through the screening response of the substrate and neighboring adatoms. Because we are not concerned with the absolute value of the binding energy, but only with coverage-dependent changes, the intra-atomic relaxation of the iodine can be left out of consideration. The dominant extra-atomic response is screening of the core hole by the conduction electrons in the surface of the substrate. The alternate extra-atomic process, the core-hole induced transfer of an electron from the substrate to the iodine, would lead to well resolved low-energy satellite structure which is not found in the present case. The well-defined asymmetry of the adsorbate line (see Table I), indicative of the metallic screening response of the substrate, offers further evidence against electron transfer, since electron transfer would obviate the need for this screening response. The observed singularity index for the adsorbate lines is actually only slightly smaller than that of the substrate  $3d$  lines. Another possible final-state effect is the polarization of neighboring adsorbate ions by the core hole, which would also cause the adsorbate core-electron binding energy to decrease with increasing coverage. However, the neighboring adsorbate atoms see not only the charge on the core ionized adsorbate atom but also the screening charge of opposite sign just below it. The field due to this dipole source is weakened and the polarization response is greatly reduced from what it would be in the absence of metallic screening. However, the polarization of neighboring adsorbate atoms may nevertheless contribute to the observed reduction of the core-electron binding energy in the ordered  $\sqrt{3} \times \sqrt{3}$  overlayer.

The dominant initial state effect arises from the electrostatic coupling to the other charged atoms in the overlayer. The change of core-electron binding energy in an ordered overlayer relative to the isolated adsorbate atom due to this interaction can be readily calculated. Using the known adsorbate atom bond length and the lattice constant of silver an upper limit for the adsorbate charge of 0.035 electron is obtained from the experimental shift, provided the entire shift is assigned to this initial state mechanism. This value can be compared to the charge transfer of 0.04 electron observed for I on Cu(001).<sup>1</sup>

Finally, it is noteworthy that the binding energy remains constant in the coverage region where the  $\sqrt{3} \times \sqrt{3}$  LEED pattern is observed. This pattern occurs well below the limiting coverage of  $\frac{1}{3}$ , in agreement with earlier work reported by Farrell.<sup>19</sup> This result is not unlike that obtained for krypton on gra-

phite which is geometrically similar in that the available sites form a triangular net with nearest-neighbor (NN) sites excluded by the size of the adsorbate atom. However, the next-nearest-neighbor (NNN) interactions are quite different because iodine, with an incomplete  $5p$  shell, will tend to become negatively charged while krypton will remain neutral. The iodine atoms will consequently have a NNN repulsive electrostatic interaction in addition to the NNN attractive van der Waals interaction which dominates in the case of krypton. Finally, in the case of a charged adsorbate ion there is an additional interaction, mediated by the substrate, due to spatial oscillations of the screening charge in the substrate. If the wavelength of the oscillations coincides with the spacing of the site of the next-nearest neighbor, that site will have an effective attractive interaction for an adsorbate atom. Consequently, the sign of the next-nearest-neighbor interaction is not known *a priori* for the adatoms of an adsorbate system.

An experimental determination of the sign of the adatom-adatom interaction requires more information than is contained in the present work. Contrary to what may seem instinctively obvious, the observed clustering does not imply that the next-nearest-neighbor interaction  $J_{NNN}$  is attractive. Preliminary Monte Carlo calculations of the dynamics of a lattice gas on a triangular lattice show that order sufficient to produce the  $\sqrt{3} \times \sqrt{3}$  LEED pattern occurs both in the low-temperature region for  $J_{NNN} < 0$ , as naively expected, and in the high-temperature region for  $J_{NNN} > 0$ . This is similar to what is known for the square lattice.<sup>20</sup> More detailed calculations of phase diagrams for the triangular lattice gas, particularly for the case of infinite nearest-neighbor repulsion, will be very helpful in interpreting experiment.<sup>21</sup> Experimentally, the sign of  $J_{NNN}$  can be most unambiguously determined by LEED observations at low temperatures, as a repulsive next-nearest-neighbor interaction should result in a  $2 \times 2$  ordering at low temperature and coverage.

#### V. CONCLUSIONS

All the results obtained here show that iodine on silver is quite distinct from iodine in the superionic conductor AgI. The adsorbate system is covalent rather than ionic, since all the evidence points to very small charge transfer to the iodine. The Ag  $3d$  spectra show neither shift nor broadening, indicating that the first atomic layer of Ag does not become distinguishable from the bulk when I is adsorbed. The valence band spectrum shows no changes toward that of AgI,<sup>22</sup> except for the inclusion of the  $I6p$  orbitals. The small shift of the I adsorbate core-electron binding energy limits the charge transfer to at most a few percent of an electron. Supporting evidence comes from the small change in work function, and from

the I-Ag distance, which is close to the sum of the Ag atomic and I covalent radii. The charge transfer is quite comparable to that observed for iodine on the (001) face of copper. The final state phenomena expected in adsorbate photoionization are also verified. The adsorbate core-electron photoemission line has

the typical many-body shape arising from the screening response of the substrate conduction electrons, and the excitation of substrate surface plasmons is confirmed. The alternative screening process, final-state charge transfer to the adsorbate atom, is apparently not important in this system.

- 
- <sup>1</sup>S. B. DiCenzo, G. K. Wertheim, and D. N. E. Buchanan, *Phys. Rev. B* (in press).
- <sup>2</sup>B. Gumhalter and D. M. Newns, *Phys. Lett. A* **53**, 137 (1975); **57**, 423 (1976).
- <sup>3</sup>K. Schonhammer, and O. Gunnarsson, *Solid State Commun.* **23**, 691 (1977).
- <sup>4</sup>J. W. Gadzuk and S. Doniach, *Surf. Sci.* **17**, 427 (1978).
- <sup>5</sup>F. Forstmann, W. Berndt, and P. Buttner, *Phys. Rev. Lett.* **30**, 17 (1973).
- <sup>6</sup>P. H. Citrin, P. Eisenberger, and R. C. Hewitt, *Phys. Rev. Lett.* **41**, 309 (1978).
- <sup>7</sup>J. H. Scofield, *J. Electron Spectrosc.* **8**, 129 (1976).
- <sup>8</sup>J. C. Riviere, *Contemp. Phys.* **14**, 513 (1973).
- <sup>9</sup>S. Doniach and M. Sunjic, *J. Phys. C* **3**, 285 (1970).
- <sup>10</sup>P. H. Citrin, G. K. Wertheim, and Y. Baer (unpublished).
- <sup>11</sup>A. Barrie and N. Christenson, *Phys. Rev. B* **14**, 2442 (1976).
- <sup>12</sup>G. K. Wertheim and P. H. Citrin, in *Photoemission in Solids, I*, edited by M. Cardona and L. Ley (Springer, Berlin, 1978).
- <sup>13</sup>C. W. Bates, Jr., G. K. Wertheim, and D. N. E. Buchanan, *Phys. Lett. A* **72**, 178 (1979).
- <sup>14</sup>J. Geiger and K. Wittmaack, *Z. Phys.* **195**, 44 (1966).
- <sup>15</sup>J. Daniels, *Z. Phys.* **203**, 235 (1967).
- <sup>16</sup>J. C. Fuggle, E. Umbach, and D. Menzel, *Solid State Commun.* **27**, 65 (1978).
- <sup>17</sup>G. K. Wertheim, *Mater. Sci. Eng.* **42**, 85 (1980).
- <sup>18</sup>J. J. Pireaux, J. Ghijsen, J. W. McGowan, J. Verbist, and R. Caudano, *Surf. Sci.* **80**, 488 (1979).
- <sup>19</sup>H. H. Farrell, M. M. Traum, N. V. Smith, W. A. Royer, D. P. Woodruff, and P. D. Johnson, *Surf. Sci.* **102**, 527 (1981).
- <sup>20</sup>K. Binder and D. P. Landau, *Surf. Sci.* **61**, 577 (1976).
- <sup>21</sup>D. P. Landau (private communication).
- <sup>22</sup>M. G. Mason, *Phys. Rev. B* **11**, 5094 (1975).